A New Resynchronization Signal Design for Rel-15 LTE-M

Amr Abdelnasser, Lutz Lampe, and Gustav Vos*
University of British Columbia, Canada, *Sierra Wireless, Canada

***Abstract*—Minimizing the resynchronization time in Long-Term Evolution for Machine Type Communications (LTE-M) is highly desirable to enhance the battery lifetime of low-power and possibly deep-coverage user equipments (UEs) targeting Internet-of-Things (IoT) applications. This has led the 3rd Generation Partnership Project (3GPP) to initiate a work item in Rel-15 LTE-M to improve cell search and/or system information acquisition time. This has been accomplished by developing a new resynchronization signal (RSS) that can be detected during relatively short device wake-up times and with low computational effort. In this paper, we review the design aspects that have been considered while deriving the new RSS signal and describe the RSS design that has been adopted by 3GPP. Moreover, we propose another RSS design and show the differences between the proposed design and the one adopted by 3GPP in terms of the detection performance and the computational and memory complexity. Finally, we highlight the gains resulting from employing the new RSS design compared to the legacy synchronization signals.**

***Keywords*:- Internet of things (IoT), 3rd generation partnership project (3GPP), Rel-15 long-term evolution for machine type communications (Rel-15 LTE-M), resynchronization signal, power consumption.**

I. Introduction

The Internet of Things (IoT) refers to billions of physical devices around the world that are capable of connecting to the Internet. Due to the availability of cheap processors and the ubiquity of wireless networks, it is possible to turn anything that can gather and transmit data, including wearables, meters, lamp-posts, smart appliances, vehicles, tablets, smart-phones, smart transportation system, etc., into part of the IoT. IoT will have huge applications that will bring immense value into our daily lives [1], [2].

IoT user equipments (UEs) are generally low-cost devices with low computation power. In addition, most of them will be battery operated. Hence, energy consumption is a critical issue. Moreover, many IoT UEs will be in locations with poor coverage conditions which represents a big challenge for massive IoT connectivity [3].

To realize an IoT in which the aforementioned requirements can be met, the 3rd Generation Partnership Project (3GPP) introduced a narrowband Long-Term Evolution (LTE) IoT technology in LTE Rel-13: LTE for Machine Type Communications (LTE-M) [4]. LTE-M is an evolution of LTE that is optimized for IoT and operates on a bandwidth (BW) of 1.08 MHz. Like LTE, LTE-M uses orthogonal frequency division multiplexing (OFDM) in downlink (DL) and single carrier frequency division multiple access (SCFDMA) in uplink (UL). In 3GPP technical specifications, an LTE-M UE is referred to as bandwidth reduced low complexity/coverage enhancement (BL/CE) UE. By using a narrowband operation, LTE-M can achieve lower costs and energy consumption compared to legacy LTE. In addition, in order to guarantee long battery lifetime, LTE-M employs extended discontinuous reception (eDRX) and power saving mode (PSM) as power saving mechanisms [5]. eDRX is a mechanism where a device sleeps by switching off part of its circuitry and decides how often to wakeup (every 5.12 s to 43.69 min) to listen for paging messages. PSM allows a device to power off and stay dormant for long periods of time (up to 413 days). Hence, PSM renders a device unreachable. Therefore, eDRX is suitable for device-terminated applications, whereas PSM is best suited for device-originated ones.

To acquire the initial time and frequency system synchronization, an LTE-M UE uses the existing LTE Primary Synchronization Signal (PSS) and Secondary Synchronization Signal (SSS) [6]. However, as a result of the sleep operation enforced by the power saving mechanisms, a clock drift will take place, which will cause the LTE-M UE to lose its acquired time and frequency synchronization. Hence, time and frequency *resynchronization* will generally be required. It was reported in [7] that a UE at extended coverage conditions would require 1.13 s on average (880 ms to detect the PSS/SSS $+$ 250 ms to decode the Physical Broadcast Channel (PBCH) to know the system frame number (SFN)) to acquire time and frequency resynchronization using the legacy synchronization signals. This long resynchronization delay causes a significant drain on battery energy due to signal processing in the wake-up state. Therefore, in Rel-15 LTE-M, 3GPP initiated the work item (WI) "Even further enhanced MTC (efeMTC) for LTE" [8], where one of the objectives was to reduce the BL/CE UEs system acquisition time. This led to the specification of a new resynchronization signal (RSS) that is denser in time and frequency than the legacy PSS/SSS and that is sent infrequently, which the UE can use for fast time and frequency resynchronization.

In this paper, we review the design aspects that have been considered in the development of the new RSS in Rel-15 LTE-M. For this purpose, we describe the RSS design that has been adopted by 3GPP. In addition, we propose an alternative RSS design that has a different design philosophy. We outline the differences between the two designs and compare their performances through simulations and analysis. In particular,

This work has been supported by Sierra Wireless and the Natural Sciences and Engineering Research Council of Canada (NSERC).

we illustrate the trade-off between computational complexity vs. cross-correlation performance and memory access rate achieved by the two designs. Finally, we show the performance gain resulting from adopting the newly proposed RSS compared to the legacy PSS/SSS, where the resynchronization time was dramatically reduced from 1.13 s to 22.6 ms.

The key contributions of this paper can be summarized as follows:

- We emphasize on the importance of properly designing an RSS that can be detected by an LTE-M UE with low computational effort.
- We make the design considerations for RSS in 3GPP available to a wide audience by explaining how the RSS was constructed, in terms of its bandwidth and duration, and the implications of the design choices on the UE computational complexity.
- We discuss the RSS design that was adopted by 3GPP.
- We further propose an alternative RSS design and highlight the trade-offs in performance offered by the two RSS designs.
- We show the performance gains resulting from the adopted RSS (compared to legacy synchronization signals) in terms of reduced energy consumption and shorter resynchronization time.

The rest of this paper is organized as follows. A background is provided in Section II. In Section III, we provide a critical review of the important aspects for the RSS design. The RSS design that was adopted in 3GPP, as well as our proposed RSS design are described in Section IV and a quantitative comparison of their performance features is presented in Section V. Section VI discusses the obtained results and concluding remarks are offered in Section VII.

II. Background

The LTE-M technology employs the same numerology as LTE and organizes its information as a function of time and frequency using a resource grid which is composed of OFDM symbols and subcarriers. The basic unit in a resource grid is referred to as a resource element (RE), which spans one symbol by one subcarrier. The available BW in LTE-M is 1.08 MHz which is divided into 6 physical resource blocks (PRBs). Each PRB is 180 kHz wide and is a contiguous set of 12 subcarriers with a subcarrier spacing of $\Delta f = 15$ kHz. Transmission in time is organized into sub-frames, where each sub-frame is 1 ms long and each 10 sub-frames make up one radio frame. Each sub-frame contains 14 OFDM symbols, of which the first 3 symbols are reserved for control information.

In Rel-15 LTE-M, the RSS will be M sub-frames long, where M is a configurable parameter that depends on the targeted coverage level (usually expressed in terms of maximum coupling loss (MCL)). Fig. 1 shows the available REs in an LTE-M resource grid for the RSS to occupy, where the RSS can only start with the 4^{th} symbol in a sub-frame.

The RSS will generally be a sequence of complex symbols that will be mapped to the available REs in the LTE-M resource grid. Let x_{RSS} be the transmitted RSS baseband OFDM signal. The received sample $y(n)$ is given by

$$y(n) = (x_{\text{RSS}} * h)(n)\, e^{j2\pi\varepsilon n/N} + w(n), \tag{1}$$

where h is the impulse response of the multipath channel, ε is the normalized frequency offset (FO) with respect to the subcarrier spacing, N is the fast Fourier transform (FFT) size, w represents the additive white Gaussian noise (AWGN), and $*$ represents the linear convolution operation.

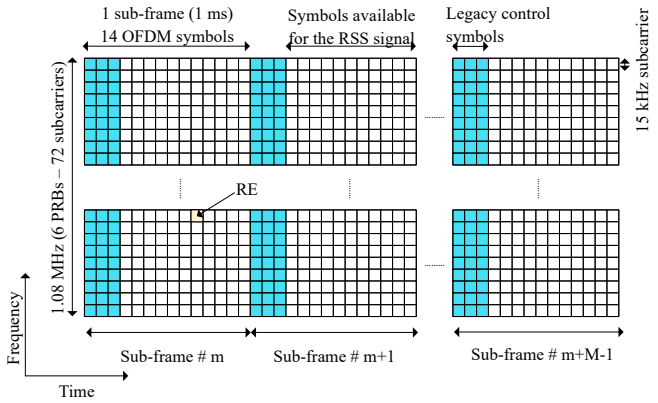

Fig. 1: The available REs for an M sub-frames long RSS in an LTE-M resource grid.

III. The Re-synchronization Signal Design Considerations

We now discuss the RSS signal detection and its design aspects. To detect an RSS and determine its beginning (symbol timing), a two-dimensional search over frequency (via frequency hypotheses) as well as time (via cross-correlations) is usually carried out at the UE between the received signal y and a local reference RSS copy x_{RSS}. Moreover, for a certain FO hypothesis and to minimize the effect of residual FO, L-part correlation [9], rather than direct correlation, is used. Assuming the RSS is composed of M sub-frames and that there are N_{s} samples per sub-frame, in the L-part correlation technique, the two signals y and x_{RSS} are both divided into L segments such that the phase change $\left(\frac{2\pi\varepsilon_{\text{r}}}{N}\frac{MN_{\text{s}}}{L}\right)$ due to the residual FO ε_{r} during the l^{th} segment duration is less than π. Hence, the cross-correlation output for a certain timing hypothesis d and frequency hypothesis ε_{h} can be written as

$$z(d,\varepsilon_{\text{h}}) = \sum_{l=1}^{L}\left|\sum_{n=(l-1)\frac{MN_{\text{s}}}{L}+1}^{l\frac{MN_{\text{s}}}{L}} y(d+n)\, x^{*}_{\text{RSS}}(n) e^{-j2\pi\varepsilon_{\text{h}} n/N}\right|^2, \tag{2}$$

where $(.)^*$ is the complex conjugate operator. In (2), we have coherent combining within a segment l and non-coherent combining among the L segments. Then the maximum likelihood estimates for the symbol timing $\hat{d}$ and the frequency offset $\hat{\varepsilon}_{\text{h}}$

are obtained as

$$\left(\hat{d}, \hat{\varepsilon}_{\mathrm{h}}\right) = \arg\max_{d,\varepsilon_{\mathrm{h}}}\{z\left(d, \varepsilon_{\mathrm{h}}\right)\}. \tag{3}$$

Also, to guarantee the existence of an RSS in the received signal y, $z\left(\hat{d}, \hat{\varepsilon}_{\mathrm{h}}\right)$ should be greater than or equal to a detection threshold λ_{th} that is set according to a target false alarm rate.

We note that all the computation burden for accurately detecting the RSS lies on the UE. Hence, the RSS attributes have to be tailored to meet the UEs' capabilities in terms of computational complexity and memory constraints as will be discussed in the following.

A. The RSS Bandwidth

If the RSS occupied the full 6 PRBs, an LTE-M UE would need to use a sampling rate of 1.92 MHz for detecting[1]. A smaller BW and thus a lower sampling rate would however reduce the computational complexity at the UE. Moreover, an RSS that occupies less BW than the 6 PRBs can be easily power spectral density (PSD) boosted[2]. However, the RSS BW cannot be too narrow, as it would lose adequate frequency diversity. According to simulations results in [10], it was found that an RSS that is 2 PRBs wide would strike a good balance between computational complexity and sufficient frequency diversity.

B. The RSS Construction in Time Domain

Considering the correlation operations in (2) for each time and frequency hypothesis considered in (3), a UE will have to perform a number of complex multiplications and additions that is proportional to the RSS length. However, to serve UEs at poor coverage conditions, hence very low signal to noise ratio (SNR) values, the RSS can be very long. For instance, for a 164 dB target MCL, the RSS can be as long as 40 ms [10]. Detecting an arbitrarily designed 40 ms RSS can easily become prohibitive in terms of UE complexity. Hence, to reduce the number of computations per time hypothesis, the following design philosophy has been adopted when constructing the RSS. A base sequence r, that occupies S consecutive OFDM symbols, is repeated to form the desired RSS length of $11M$ OFDM symbols. This approach reduces the computations required per timing hypothesis significantly, since it is possible to derive the cross-correlation result at a certain hypothesis by making use of the cross-correlation result at a previous hypothesis. Fig. 2a illustrates this idea by showing the cross-correlation between an incoming signal and a local reference RSS that is formed by the repetitions of the base sequence r. At the timing hypothesis d_m, the cross-correlation result is

$$\begin{aligned} & z\left(d_m, \varepsilon_{\mathrm{h}}\right) \\ &= y_{m+1}(r^*)^T + y_m(r^*)^T + y_{m-1}(r^*)^T + y_{m-2}(r^*)^T, \end{aligned} \tag{4}$$

where y_m is a vector of received samples matched to the length of r and $(.)^T$ is the transpose operator. At the timing hypothesis d_n, the cross-correlation result is

$$\begin{aligned} & z\left(d_n, \varepsilon_{\mathrm{h}}\right) \\ &= y_{m+2}(r^*)^T + y_{m+1}(r^*)^T + y_m(r^*)^T + y_{m-1}(r^*)^T \\ &= y_{m+2}(r^*)^T + z\left(d_m, \varepsilon_{\mathrm{h}}\right) - y_{m-2}(r^*)^T. \end{aligned} \tag{5}$$

Hence, a UE does not need to perform the cross correlation between the received RSS and the whole reference RSS copy stored in its memory. The UE can rather cross-correlate the received RSS with just the shorter base sequence r and, by properly adding the correlation results, can still arrive at the overall cross-correlation result.

However, some method should be considered to make the base sequence r repetitions different from each other to eliminate false detections. Otherwise, a UE may wrongly detect the beginning of the RSS sequence which can cause serious timing error. Hence, a cover code (CC) is used to control how the base sequence fills the sub-frames. Two approaches were proposed in 3GPP, where, according to the CC, $\{r, -r\}$ and $\{r, r^*\}$ will be filling the sub-frames.

Fig. 2b shows an example for a reference sequence $\{+r, -r, +r\}$. The overall cross-correlation peak $3\left\|r\right\|^2$, where $\|.\|$ is the L2-norm, can be obtained by cross-correlating the incoming sequence with the full length sequence (as shown in the left part of the figure) or by cross-correlating the incoming sequence with just the base sequence $+r$ and applying the CC $\{+1, -1, +1\}$ to the correlation result $\{\left\|r\right\|^2, -\left\|r\right\|^2, \left\|r\right\|^2\}$ (as shown in the right part of the figure). Similar techniques can be followed with the $\{r, r^*\}$ approach, where the cross-correlations have to be now done with both r and r^*. Notice that the base sequence r can vary in length. For a given RSS length, as the base sequence gets longer, the CC gets shorter and vice versa.

C. Computational Complexity and Memory Access Requirements

In some UE implementations, the correlation results with the base sequence are stored in an off-chip external memory [11]. Then, for each time hypothesis, those correlation results are invoked from the external memory and the CC is applied to them to constitute the overall cross correlation result. In this context, the base sequence and the CC lengths affect the computational complexity and the read rate from the external memory differently.

Fig. 2c gives an example of two RSS designs that adopt the base sequence approach. Both designs have the same length and occupy the same BW, hence use the same sampling rate. However, Design #1 has a 3 times longer base sequence r and a 3 times shorter CC than Design #2. As a result, Design #1 requires a higher number of computations (multiplications and

[1]In LTE, the used sampling frequency f_{s} is related to the subcarrier spacing as follows: $f_{\mathrm{s}} = N\Delta f$. If the RSS occupies 6 PRBs, N will be 128 which will result in $f_{\mathrm{s}} = 128 \times 15 \times 10^3 = 1.92$ MHz.

[2]PSD boosting is a technique used by the eNodeB (eNB) in DL transmissions to UE devices. The eNB allocates more power to some PRBs, which effectively improves their coverage. This will, however, leave the other PRBs blocked, i.e. with no power allocated.

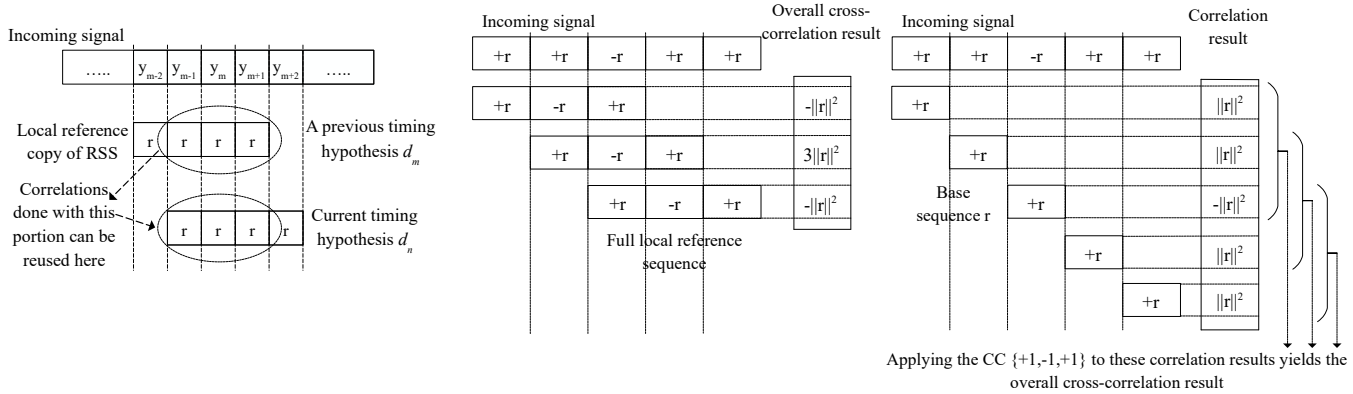

(a) Exploiting the repetitions in the RSS design can save computations.

(b) Obtaining the overall cross-correlation result by cross-correlating with the full sequence vs. cross-correlating with the base sequence r.

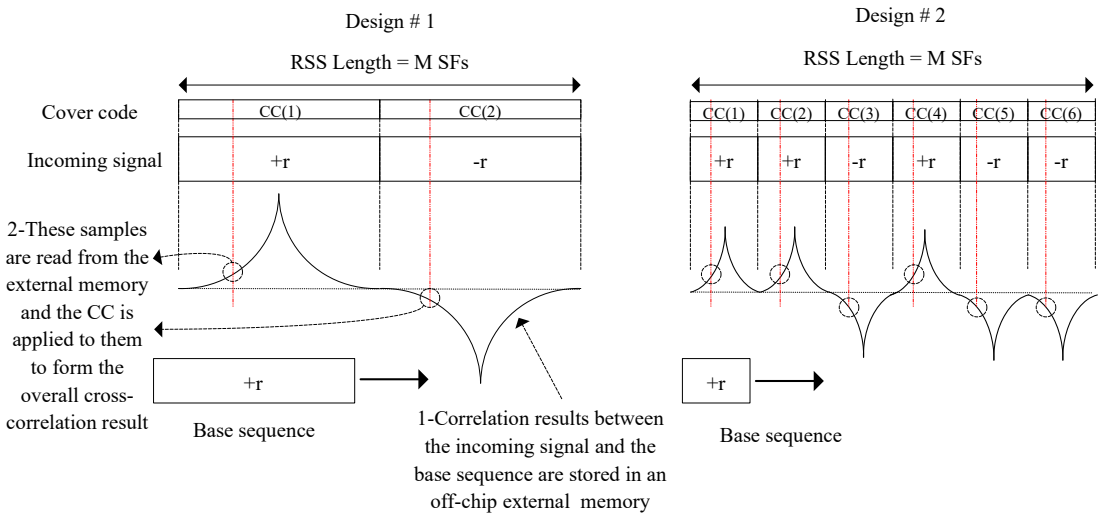

(c) Two designs that adopt the base sequence approach. Design #1 has longer base sequence r and shorter CC, whereas Design #2 has shorter base sequence r and longer CC.

Fig. 2: The base sequence approach.

additions) per time hypothesis but a lower memory read-rate. Only 2 samples need to be read from the external memory at a certain time hypothesis to apply the CC to for Design #1, whereas Design #2 needs 6 samples to be read from memory to apply the CC to. Hence, in that specific example, Design #2 has a memory read rate that is 3 times that of Design #1. Therefore, Design #1 is more suitable for UEs that have stringent constraints on memory access rate, whereas Design #2 is more suitable for UEs that have less computational power.

D. Information Content

Beside its use for re-acquiring system timing and frequency synchronization, the RSS should provide information about the cell identity (ID), so that a UE can verify that it is actually trying to resynchronize to the same cell it is currently camping on. In addition, the RSS should be capable of indicating if there is any change in system information so that a UE may skip decoding the PBCH. Hence, each cell needs two unique RSSs, and since we have 504 different cell-IDs, we need a total of $504 \times 2 = 1008$ unique RSS sequences. These sequences must have sufficient distinguishability from each other, meaning that they should have good cross-correlation properties. Otherwise, RSSs belonging to different cells may severely interfere with each other and hinder the RSS detection process.

IV. RSS Designs

In this section, we describe two RSS designs, one that was adopted in 3GPP [12], [13] and an alternative one that we proposed in [14], where both designs follow the principles outlined earlier.

A. Long Base Sequence with Short Cover code: Design A

This design was originally presented in [11] and was adopted in 3GPP [12], [13], where the RSS is constructed by using a base sequence r that occupies 11 consecutive symbols. The base sequence is formed using a 24 sub-carriers $\times$ 11 symbols $\times$ 2 = 528 elements long Gold sequence which is

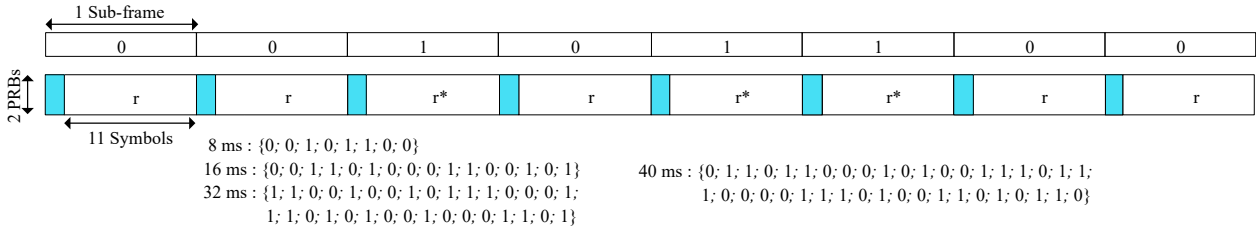

(a) Design A using the cover code $\{0, 0, 1, 0, 1, 1, 0, 0\}$ for the 8 ms RSS and the cover codes for the different RSS lengths.

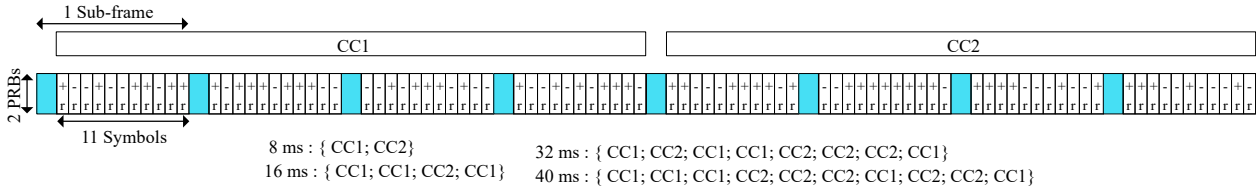

(b) Design B using the cover code $\{\text{CC1}, \text{CC2}\}$ for the 8 ms RSS and the cover codes for the different RSS lengths.

Fig. 3: The base sequence placement for the two 8 ms RSS alternatives and the cover codes used for the different RSS lengths.

initialized by $c_{\text{init}} = N_{\text{ID}}^{\text{cell}} + 2^9 u$, where $N_{\text{ID}}^{\text{cell}}$ is the physical cell-ID and u is a flag that is used to indicate whether there is a change in the system information or not. This way, 1008 different RSSs can be produced. The 528 elements long sequence is then mapped to 264 quaternary phase shift keying (QPSK) symbols occupying 24 sub-carriers $\times$ 11 symbols. The base sequence r is then repeated in subsequent sub-frames according to a binary cover code, where a 0 means that the sequence r will be used to fill the corresponding sub-frame, whereas a 1 means that the complex conjugate of the sequence r will be used to fill the corresponding sub-frame until the desired RSS length is reached. Fig. 3a shows the base sequence r placement for the 8 ms RSS, as well as, the cover codes corresponding to 4 possible RSS lengths. The cover codes were specified such that the RSSs have the lowest possible side-peaks in their auto-correlation functions. Design A falls under Design #1 category.

B. Short Base Sequence with Repeated Short Cover Codes: Design B

In [14], we proposed an alternative RSS design which is constructed as follows. Different from the previous design, the base sequence r occupies one symbol. It is formed using a 24 elements long truncated Zadoff-Chu (ZC) sequence (truncated from a 101 elements long ZC sequence). The base sequence is then repeated in subsequent symbols according to a bi-polar cover code, where a 1 in the cover code means that r will occupy the corresponding symbol, whereas a -1 means that $-r$ will occupy the corresponding symbol, until the desired RSS length is reached. However, instead of using an $11M$ elements long cover code for the base sequence placement (which was shown earlier in Design #2 to lead to a high memory access rate), another approach was followed. A shorter cover code is used that is then repeated to reach the desired length ($11M$). The cover codes for the different RSS lengths are shown in Fig. 3b. As is clear for the 16, 32, and 40 ms designs, two 44 elements long cover codes (CC1 and CC2) are used and repeated. This will reduce the number of computations as well as the memory access rate by the factor of repetitions (by a factor of 2 for the 16 ms RSS, a factor of 4 for the 32 ms case, and a factor of 5 for the 40 ms case). The reduction comes from the fact that, to form the overall cross-correlation results, the repeated parts of the CC can benefit from the earlier application of the original parts of the CC to the correlation results.

The repetitions of the cover codes were done in a way such that the side-peaks of the autocorrelation function of the RSSs are as low as possible. Using the generator polynomials $x^6 + x + 1$ and $x^6 + x^5 + x^2 + x + 1$, 28 truncated gold sequences of length 44 elements and $< 40\%$ normalized cross-correlations were easily obtained. Hence, there are $28/2 = 14$ pairs of cover codes (CC1 and CC2). Together with up to 100 possible ZC sequences, 1008 different RSSs can be obtained. Fig. 3b shows the base sequence r placement for the proposed 8 ms RSS. Design B falls under Design #2 category.

V. Comparison Between the Two RSS Designs

We now provide a comparison between the performances of the two RSS designs. Simulations in this section were conducted using Matlab [15] according to the simulation parameters listed in Table I [14].

A. Cross-Correlation Performance of the RSSs

Fig. 4 studies the cumulative density function (CDF) of the cross-correlation performance between 1008 RSS 8 ms sequences for the two designs. For both schemes, for 90% of the cases, the normalized cross-correlation peak will be ≤ 0.12. However, for Design A, the maximum normalized cross-correlation peak is about 0.2, whereas it is almost 0.5 for Design B. The cross-correlation performance and consequently the interference level between the RSS sequences can be

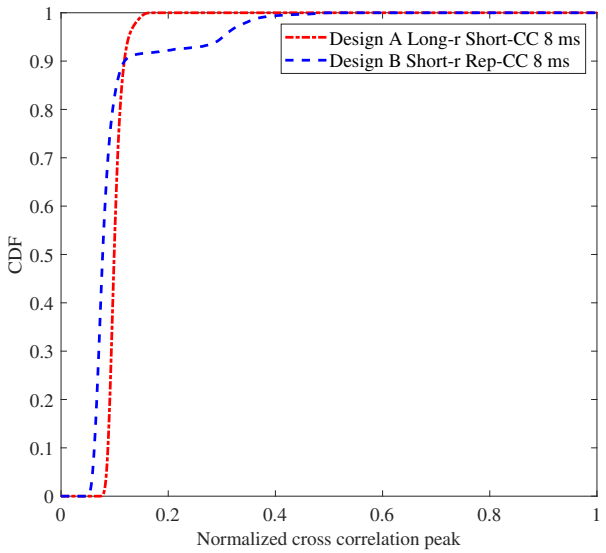

Fig. 4: The CDF of the normalized cross-correlation between 1008 RSS sequences for the two designs.

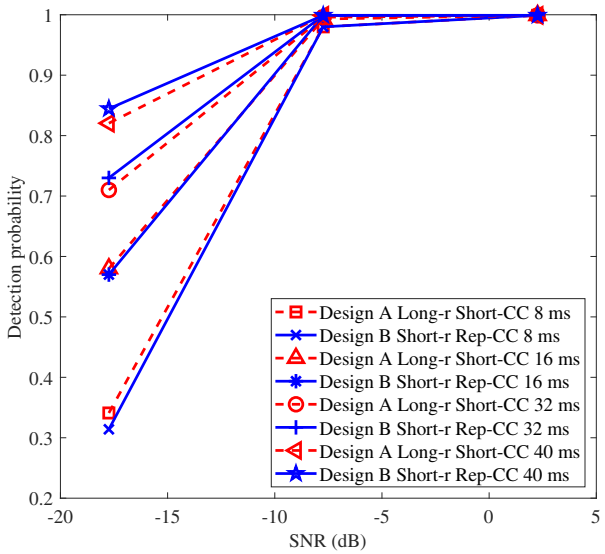

Fig. 5: The detection probabilities of the two designs for the 8, 16, 32, and the 40 ms signal durations.

improved by transmitting different sets of RSSs on different frequencies, since the cross-correlation analysis in Fig. 4 assumed that the 1008 RSS sequences are all transmitted on the same frequency, which is a pessimistic scenario.

B. Computation Complexity and Memory Access Rate

Table II compares between the two designs in terms of the number of million operations per second (MOPS) and the memory access rate for the 40 ms RSS, assuming that 10 frequency hypotheses are performed in (3). The MOPS calculations account for the computations required to perform the cross-correlation with the base sequence, using an efficient overlap-and-add implementation [16], as well as the application of the cover code to obtain the overall cross-correlation result. While Design A has lower memory access rate, Design B requires less MOPS and, consequently, lower computational complexity.

TABLE I: Simulation parameters

Parameter	Value
eNB transmit (Tx) antenna configuration	2 Tx antennas
UE receive (Rx) antenna configuration	1 Rx antenna
eNB Tx power	46 dBm per Tx port
eNB antenna switching period	2 ms
System bandwidth	10 MHz
Band	Band 8 (900 MHz)
Channel model	Extended Typical Urban
Doppler spread	1 Hz
UE noise figure	9 dB
PSD boosting	$10\log_{10} 3 = 4.7$ dB
Carrier frequency offset (CFO)	$[-4.5$ kHz : 4.5 kHz$]$
Average residual CFO after 10 frequency hypotheses	225 Hz
Coherent combining duration	1 ms
Detection threshold λ_{th}	Set for false alarm rate $= 0.1\%$
Detection window	± 3.5 μs around the true timing

C. Detection Performance of the RSSs

Fig. 5 studies the detection performance of the two RSS designs for the 8, 16, 32, and the 40 ms signals assuming a PSM sleep time of 4 hours. The detection probability is defined as the probability that the detected correlation peak (which is indicative of the beginning of the RSS signal) lies within a window of ± 3.5 μs around the true timing (actual beginning of the RSS signal). The detection performance of the two RSS designs was studied at SNR values of -17.74 dB, -7.74 dB, and 2.26 dB which correspond to MCL values of 164 dB, 154 dB, and 144 dB, respectively. It is clear from Fig. 5 that the two RSS designs enjoy similar detection performance. Also, as expected, the detection probability increases as the RSS length increases. Moreover, it was shown in [10] that by applying a $10\log(3) = 4.7$ dB PSD boost to the 2-PRB RSS signals, it was possible to attain a comparable detection performance to an RSS that would occupy the full 6 PRBs.

TABLE II: Computational complexity and memory access rate for the 40 ms RSS

Performance criterion	Design A Long r, short CC	Design B Short r, repeated CC
Computational complexity (MOPS)	943	754
Memory access rate (Msps)	192	422

TABLE III: Average resynchronization times (ms) using the RSS and the legacy PSS/SSS for eDRX scenarios B and C

eDRX cycle (s)	RSS Length (ms)			Legacy PSS/SSS	
	16	32	40	No boost	4 dB boost
B - 20.48	16.4	32.4	40.4	880	220
C - 327.68	22.6	38.6	46.6	1130	345

VI. Discussion

While having similar detection performance, Design A was shown to have better overall cross-correlation performance, lower memory access rate, but higher computational complexity than Design B. Hence, Design A is more suitable for UEs that have memory with tight read rate constraints, whereas Design B is more suitable for UEs with more emphasis on limited computational power.

Now, using Design A, Table III shows the average resynchronization times at a 164 dB target MCL for different eDRX scenarios [17] and different RSS lengths. Note that, for scenario-C and due to the timing error exceeding half the PSS/SSS period, a UE, using the legacy PSS/SSS, will have to decode the PBCH as well to know the SFN. This is not the case for the RSS due to its long periodicity [12]. The average resynchronization times range from 16.4 ms to 46.6 ms, which is a huge reduction compared to an average resynchronization time that ranges from 880 ms to 1.13 s or from 220 ms to 345 ms with a 4 dB DL PSD boosting [7] using the legacy synchronization signals. Since the UE energy consumed during the resynchronization operation is directly proportional to the average resynchronization time, a reduction in the resynchronization time, for example, from 1.13 s to 22.6 ms can lead to up to 98% savings in the UE energy consumption.

VII. Conclusion

In Rel-15 LTE-M, 3GPP has dedicated a significant effort on designing a new resynchronization signal in order to minimize system acquisition time. This is foreseen to minimize the UEs' energy consumption as well. In this context, two practical low complexity RSS designs (Design A and Design B) were studied in this paper. In the two designs, computational complexity was reduced by decreasing the RSS bandwidth while maintaining sufficient frequency diversity. In addition, it was possible to further reduce the computational complexity by adopting a base sequence topped with a cover code approach. Simulated performance results confirmed the efficacy of the newly proposed RSS by showing how the resynchronization times were greatly reduced when compared to the legacy PSS/SSS.

We believe that the work presented in this paper makes the design considerations for RSS in 3GPP available to a wide audience and provides a balanced evaluation and insights into the effectiveness of the design choice. We also expect that this work can be a meaningful starting point for related design tasks in other system standards for low-complexity IoT devices possibly operating in deep coverage.

References

[1] A. Al-Fuqaha, M. Guizani, M. Mohammadi, M. Aledhari, and M. Ayyash, "Internet of things: A survey on enabling technologies, protocols, and applications," *IEEE Communications Surveys Tutorials*, vol. 17, pp. 2347–2376, Fourthquarter 2015.

[2] N. Neshenko, E. Bou-Harb, J. Crichigno, G. Kaddoum, and N. Ghani, "Demystifying IoT security: An exhaustive survey on IoT vulnerabilities and a first empirical look on internet-scale IoT exploitations," *IEEE Communications Surveys Tutorials*, vol. 21, pp. 2702–2733, thirdquarter 2019.

[3] G. A. Akpakwu, B. J. Silva, G. P. Hancke, and A. M. Abu-Mahfouz, "A Survey on 5G Networks for the Internet of Things: Communication Technologies and Challenges," *IEEE Access*, vol. 6, pp. 3619–3647, 2018.

[4] A. Rico-Alvarino, M. Vajapeyam, H. Xu, X. Wang, Y. Blankenship, J. Bergman, T. Tirronen, and E. Yavuz, "An overview of 3GPP enhancements on machine to machine communications," *IEEE Communications Magazine*, vol. 54, pp. 14–21, June 2016.

[5] 3GPP TS 24.008, "Mobile radio interface Layer 3 specification; Core network protocols; Stage 3," V.16.3.0, Dec. 2019.

[6] C. Cox, *An Introduction to LTE: LTE, LTE-Advanced, SAE, VoLTE and 4G Mobile Communications*. Wiley, 2nd ed., 2014.

[7] Sierra Wireless, Ericsson, Altair, Sony, Virtuosys, AT&T, Verizon, Orange, Nokia, China unicom, Docomo, KDDI, kpn, KT, Sequans, SK Telecom, Singtel, SoftBank, Sprint, telenor, "Evaluation of LTE-M towards 5G IoT requirements," *White Paper*, pp. 1–20, 2018, https://altair-semi.com/wp-content/uploads/2018/03/LTE-M-Performance-Towards-5G-White-Paper-V1.1-Final.pdf.

[8] Ericsson and Qualcomm Inc., "New WID on Even further enhanced MTC for LTE," in *3GPP TSG RAN Meeting # 75, Dubrovnik, Croatia, Tech. Rep. RP-170732*, pp. 1–4, Mar 2017.

[9] J. G. Proakis, *Digital Communications*. McGraw-Hill, 2014.

[10] Qualcomm Inc., "Reduced system acquisition time," in *3GPP TSG RAN Meeting # 92, Athens, Greece, Tech. Rep. R1-1802324*, pp. 1–10, Mar 2018.

[11] Qualcomm Inc., "Reduced system acquisition time," in *3GPP TSG RAN Meeting # 93, Busan, South Korea, Tech. Rep. R1-1807102*, pp. 1–10, May 2018.

[12] Ericsson, "Agreement summary for Rel-15 Even further enhanced MTC for LTE," in *3GPP TSG-RAN WG1 Meeting # 93, Busan, Korea, Tech. Rep. R1-1807581*, pp. 1–44, May 2018.

[13] 3GPP TS 36.211, "Technical Specification Group Radio Access Network; Evolved Universal Terrestrial Radio Access (E-UTRA); Physical channels and modulation (Release 16) ," V16.0.0, Dec. 2019.

[14] Sierra Wireless, "Resynchronization Signal Design Considerations," in *3GPP TSG RAN Meeting # 93, Busan, Korea, Tech. Rep. R1-1806002*, pp. 1–10, May 2018.

[15] The Mathworks, Inc., Natick, Massachusetts, *MATLAB R2018b*, 2018.

[16] J. G. Proakis, *Digital Signal Processing (4th edition)*. Pearson, 2006.

[17] Ericsson, "Assumptions for eMTC power consumption for power saving signal/channel," in *3GPP TSG-RAN WG1 Meeting # 90, Prague, Czech Republic, Tech. Rep. R1-1714992*, pp. 1–8, Aug 2017.